CERN-EP/82-120
6 August 1982

EUROPEAN ORGANISATION FOR NUCLEAR RESEARCH

TRANVERSE MOMENTUM SPECTRUM OF NEUTRAL ELECTROMAGNETIC PARTICLES PRODUCED AT THE CERN PROTON ANTIPROTON COLLIDER

UA1 Collaboration, CERN, Geneva, Switzerland

G. Arnison[10], A. Astbury[10], B. Aubert[2], C. Bacci[9], R. Bernabei[9], A. Bézaguet[4],
R. Böck[4], T.J.V. Bowcock[6], M. Calvetti[4], T. Carroll[4], P. Catz[2], S. Centro[4],
F. Ceradini[9], S. Cittolin[4], A.M. Cnops[4], C. Cochet[11], J. Colas[2],
M. Corden[3], D. Dallman[12], S. D'Angelo[9], M. DeBeer[11], M. Della Negra[2], M. Demoulin[4],
D. Denegri[11], D. DiBitonto[4], L. Dobrzynski[7], J.D. Dowell[3], M. Edwards[3],
K. Eggert[1], E. Eisenhandler[6], N. Ellis[3], P. Erhard[1], H. Faissner[1], G. Fontaine[7],
J.P. Fournier[11], R. Frey[8], R. Frühwirth[12], G. Garvey[3], S. Geer[7], C. Ghesquière[7],
P. Ghez[4], K.L. Giboni[1], W.R. Gibson[6], Y. Giraud-Heraud[7], A. Givernaud[11],
A. Gonidec[2], G. Grayer[10], P. Gutierrez[8], R. Haidan[4], T. Hansl-Kozanecka[1],
W.J. Haynes[10], L.O. Hertzberger*, C. Hodges[8], D. Hoffmann[1], H. Hoffmann[4],
D.J. Holthuizen*, R.J. Homer[3], A. Honma[6], W. Jank[4], P.I.P. Kalmus[6], V. Karimäki[5],
R. Keeler[6], I. Kenyon[3], A. Kernan[8], R. Kinnunen[5], H. Kowalski[4], W. Kozanecki[8],
D. Kryn[7], F. Lacava[4], J.P. Laugier[11], J.P. Lees[2], H. Lehmann[1], R. Leuchs[1],
A. Leveque[11], D. Linglin[2], E. Locci[11], T. Markiewicz[4], G. Maurin[4],
T. McMahon[3], J.P. Mendiburu[7], M.N. Minard[2], M. Moricca[9],
F. Muller[4], A.K. Nandi[10], L. Naumann[4], A. Norton[4], A. Orkin-Lecourtois[7],
L. Paoluzi[9], G. Piano Mortari[4], M. Pimïa[5], A. Placci[4], E. Radermacher[1],
J. Ransdell[8], H. Reithler[1], J.P. Revol[4], J. Rich[11], M. Rijssenbeek[4], C. Roberts[10],
C. Rubbia[4], B. Sadoulet[4], G. Sajot[7], G. Salvi[6], G. Salvini[9], J. Sass[11],
J. Saudraix[11], A. Savoy-Navarro[11], D. Schinzel[4], W. Scott[10], T.P. Shah[10],
M. Spiro[11], J. Strauss[12], K. Sumorok[3], F. Szoncso[12], C. Tao[4], J. Timmer[4],
G. Thompson[6], E. Tscheslog[1], J. Tuominiemi[5], J.P. Vialle[4], J. Vrana[7],
V. Vuillemin[4], H. Wahl[12], P. Watkins[3], J. Wilson[3], M. Yvert[2], E. Zurfluh[4]

Aachen[1] -Annecy (LAPP)[2]-Birmingham[3]-CERN[4]-Helsinki[5]-Queen Mary College, London[6]-Paris (Coll.de France)[7]-Riverside[8]-Roma[9]-Rutherford Appleton Lab.[10]-Saclay (CEN)[11]-Vienna[12] Collaboration

Presented to the XXI International Conference on High Energy Physics
Paris 26-31 July 1982

* NICKHEF, Amsterdam, The Netherlands

Abstract

Forward shower counters equipped with position detectors able to locate in space the centre of gravity of energetic electromagnetic showers to ± 2 mm have been used to measure an inclusive p_t distribution in the rapidity range $1.6<|y|<2.5$ for neutral electromagnetic particles produced in proton-antiproton collisions at $\sqrt{s}$=540 GeV. The covered p_t range extends up to 12 GeV/c.

The transverse momentum spectrum of charged particles produced in proton-antiproton collisions at $\sqrt{s}=540$ GeV has been measured in the UA1 experiment up to $p_t \approx 10$ GeV/c in the central rapidity region $|y| < .5$[1]. In this paper, we report on a measurement of the tranverse momentum spectrum of neutral electromagnetic particles produced at forward angles, but still in the rapidity plateau, $1.6 < |y| < 2.5$. The measurement was performed by triggering the UA1 detector on localised large transverse energy deposited in the end cap electromagnetic shower counters.

The UA1 central detector is surrounded by shower counters with fine sampling placed inside the magnet coil as shown in figure 1. The end cap electromagnetic shower counters cover both ends of the central detector at 3 metre distance from the beam crossing point. With respect to the beam axis, they cover an angular range of $5^0 < \theta < 25^0$. They consist of a sandwich of 27 radiation lengths (r.l.) of 4 mm lead sheets and 6 mm scintillator sheets. As shown on figure 2, they are subdivided into 32 identical azimuthal cells of angular size $\Delta\varphi \times \Delta\theta = 11.2^0 \times 20^0$. Each cell is subdivided in depth into four segments (4r.ℓ.,7r.ℓ.,9r.ℓ.,7 r.ℓ.). The light produced in each segment is seen by wave shifter plates at the periphery, which in turn are connected via light guides to photomultipliers located outside the magnet. The position of the shower is measured with a position detector located inside the calorimeter at a depth of 11 r.ℓ. i.e. after the first two segments. The position detector, shown in figure 2, consists of two planes of orthogonal proportional tubes of 2x2 cm^2 cross-section. The deposited charge is read on both ends of the wire of each tube, so that each plane measures independently the space position of the shower : barycentre of the tube coordinate and barycentre of the charge division coordinate. The position detector locates the centre of gravity of energetic electromagnetic showers to ± 2 mm[2] in space.

All segments have been calibrated relative to each other within ± 3% with a 4 Curie Co^{60} source moved from cell to cell along a circle of 1 m radius ; the absolute energy scale comes from the measured ratio of the response of the calorimeter to an electron beam of known energy and to the same cobalt source. Although the final calibration procedure should be more precise, the estimated uncertainty on the absolute energy scale for the data presented here is ± 5%. This uncertainty translates into a 30% uncertainty on the inclusive cross-section. The intrinsic energy resolution of the calorimeter is $15\%/\sqrt{E_t}$, where E_t is the transverse energy $E_t = E \sin\theta$.

The attenuation length of the scintillator has been chosen to match the variation of $\sin\theta$ over the radius of the calorimeter : $0.3\text{m} < r < 1.5$ m. All segments have been mapped with the cobalt source. Figure 3 shows the response of one particular segment to the cobalt source as a function of r. Up to r = 1.2 m the attenuation is exponential. The variation of $\sin\theta$ as a function of r is shown for comparison. It can be seen that without an attenuation correction the calorimeter measures the transverse energy directly to better than a factor of 2. This property was used to trigger on showers with large transverse energy. A trigger was generated whenever the sum of the signals of two adjacent azimuthal cells exceeded a given threshold. The integrated luminosities for the two thresholds used are listed in Table 1.

From a total of 5000 recorded triggers 77 neutral electromagnetic showers with $E_t > 3.8$ GeV have been reconstructed which satisfy the following criteria :

i) A vertex is found in the central detector, but no charged track points to the two triggering cells.

ii) The deposition of energy in the four segments of the two triggering cells should be compatible with the longitudinal profile of an electromagnetic shower.

iii) The position detector should show only one cluster for the two triggering cells, with a total charge deposited compatible with the energy measured in the scintillators.

Four p_t bins have been defined (see table 2). The acceptance in each bin has been evaluated using a Monte Carlo programme, assuming no direct production of single photons. A mixture $2/3\pi^0 + 1/3\eta^0$ has been generated with a p_t spectrum identical to the measured charged particle spectrum at this energy[1]. Each decay photon is tracked into the calorimeter ; photomultiplier and position detector signals are generated. An event is accepted if the above selection criteria are satisfied and if the raw "transverse energy response" is above threshold. At large transverse momenta the acceptance is close to 1 since the two decay photons always merge into one unresolved cluster. Table 2 gives the acceptances for the two different threshold values used. Finally one has to correct for the loss of π^0's or η^0's accompanied by another charged particle or another photon in the two triggering cells. Assuming charge independence, one can use the large p_t charged particle data to estimate the probability to find an isolated large p_t π^0 in the solid angle defined by the two triggering cells ; it is found to be 42% and independent of p_t. This overlap correction is dominated by random overlaps of uncorrelated soft particles. The number of correlated hard secondaries is small : less than 10% of large p_t charged hadrons are accompanied by a secondary with $p_t > 1$ GeV/c in $\Delta y \times \Delta\varphi = 1 \times 22^0$.

The invariant cross-section deduced for the reaction $pp \to h^0 + \text{anything}$, in the rapidity interval $1.6 < |y| < 2.5$, where h^0 is an unresolved mixture of π^0, η^0, γ's is given in Table 2 and displayed in figure 4 as a function of p_t (open squares). The charged particle spectrum, averaged between positive and negative particles (crosses) measured with our central detector[1] has been added for comparison on figure 2. Given that the two spectra are for different particle mixtures, the agreement is good. When comparing to ISR data in the same p_t range, we reach independently the same conclusion as with the charged particle spectrum. The yield of large p_t particles increases strongly with $\sqrt{s}$ as expected for the constituent hard scattering interpretation. At $p_t=10$ GeV/c the invariant cross-section increases by 3 orders of magnitude between $\sqrt{s}=63$ GeV and $\sqrt{s}=540$ GeV.

Acknowledgements

We should like to thank the members of the CERN Accelerator Divisions for their work in commissioning the SPS Collider and providing the collisions which have yielded this physics. We are extremely grateful to the CERN management and staff who have supported the UA1 experiment so generously, and extend these warm thanks to the following external sources of financial support :

Fonds zur Forderung der Wissenschaftlichen Forshung, Austria.
Valtion luonnontieteellinen toimikunta, Finland.
Institut National de Physique Nucléaire et de Physique des Particules and Institut de Recherche Fundamentale (CEA), France.
Bundesministerium fur Forschung und Technologie, Germany.
Istituto Nazionale di Fisica Nucleare, Italy.
Science and Engineering Research Council, United Kingdom.
Department of Energy, USA

A great deal of understanding was demanded of all these bodies in order that we could realise the UA1 detector on the timescale required. Our technical and engineering colleagues in the collaborating institutes provided the untiring support needed to build UA1 ; without their efforts we would have nothing to report, and we deeply acknowledge their work, especially those of the Annecy (LAPP) group for having built and brought the end-cap electromagnetic calorimeters into action. Thanks are also due to the following people who have worked with the collaboration in the preparation and data collection on the runs described here, D. Cline, G. Petrucci, P. Queru, M. Steuer, H. Verweij and R. Wilson.

References

1) "Transverse momentum spectrum for charged particle at the CERN proton-antiproton. Collider", UA1 Collaboration, Paper submitted to this Conference.

2) B. Aubert et al., Nucl.Instr. and Meth. 176 (1980) 195.

TABLE 1

Triggers and integrated luminosities

Trigger threshold	Number of equivalent inelastic collisions	∫L dt
E_t > 4 GeV	78,000	1.95 10^{30} cm^{-2}
E_t > 6 GeV	231,000	5.77 10^{30} cm^{-2}

TABLE 2

Invariant cross-section and acceptances for the reaction $\bar{p}p \to h^0$ + anything at $\sqrt{s}=540$ GeV in the rapidity range $1.6 < |y| < 2.5$ where h^0 is assumed to be a mixture $2/3\ \pi^0 + 1/3\ \eta^0$

p_t interval [GeV/c]	$< p_t >$ [GeV/c]	Acceptance $E_t > 4$ GeV	Acceptance $E_t > 6$ GeV	$Ed^3\sigma/dp^3$ [$cm^2\ GeV^{-2}$]
3.8 - 4.7	4.2	0.34	–	$(1.40 \pm 0.35) \times 10^{-30}$
4.7 - 7.6	5.4	0.62	–	$(2.24 \pm 0.49) \times 10^{-31}$
7.6 - 10.6	8.5	0.96	0.81	$(1.14 \pm 0.38) \times 10^{-32}$
10.6 - 13.5	11.6	0.99	0.99	$(4.32 \pm 2.16) \times 10^{-33}$

Figure captions

Fig. 1. The UA1 detector.

Fig. 2. Exploded view of the end cap electromagnetic calorimeter showing the segmentation in 32 azimuthal cells and the position detector.

Fig. 3. Response of a particular calorimeter segment to the Cobalt source as a function of r. Variation of $\sin\theta$ over the same radius range is shown for comparison.

Fig. 4. Single particle invariant cross-section as a function of p_t measured at the proton-antiproton collider and at the ISR.

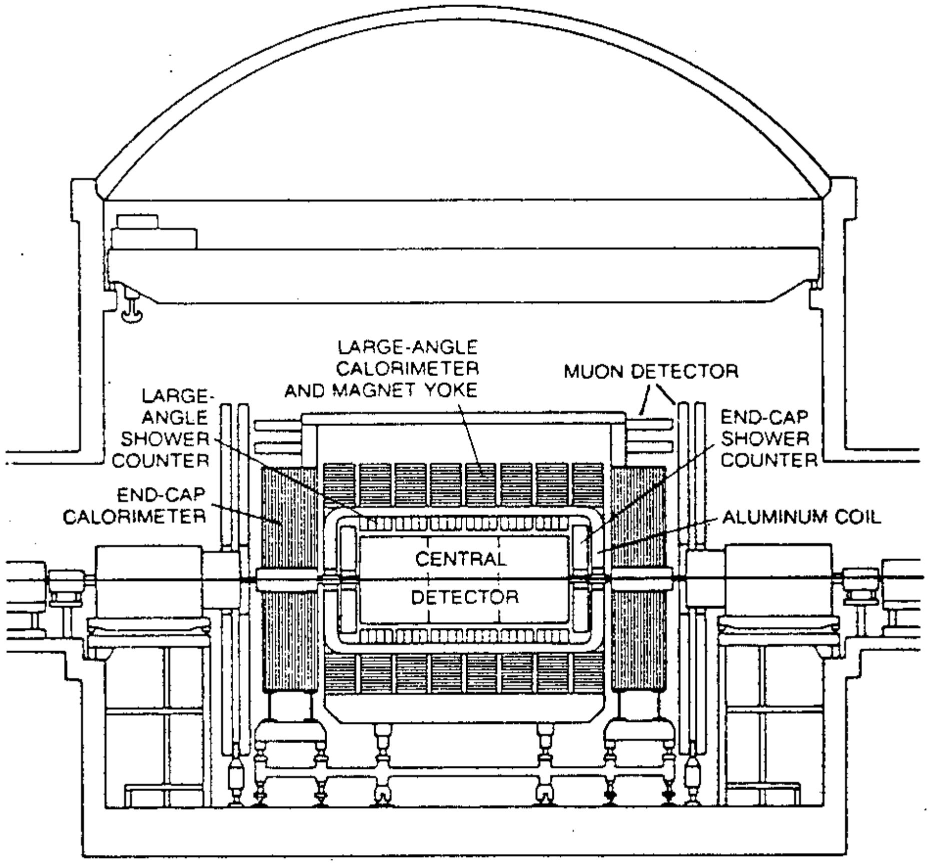
LARGE-ANGLE
CALORIMETER
AND MAGNET YOKE
MUON DETECTOR
LARGE-
ANGLE
SHOWER
COUNTER
END-CAP
SHOWER
COUNTER
END-CAP
CALORIMETER
ALUMINUM COIL
CENTRAL
DETECTOR

Fig. 1

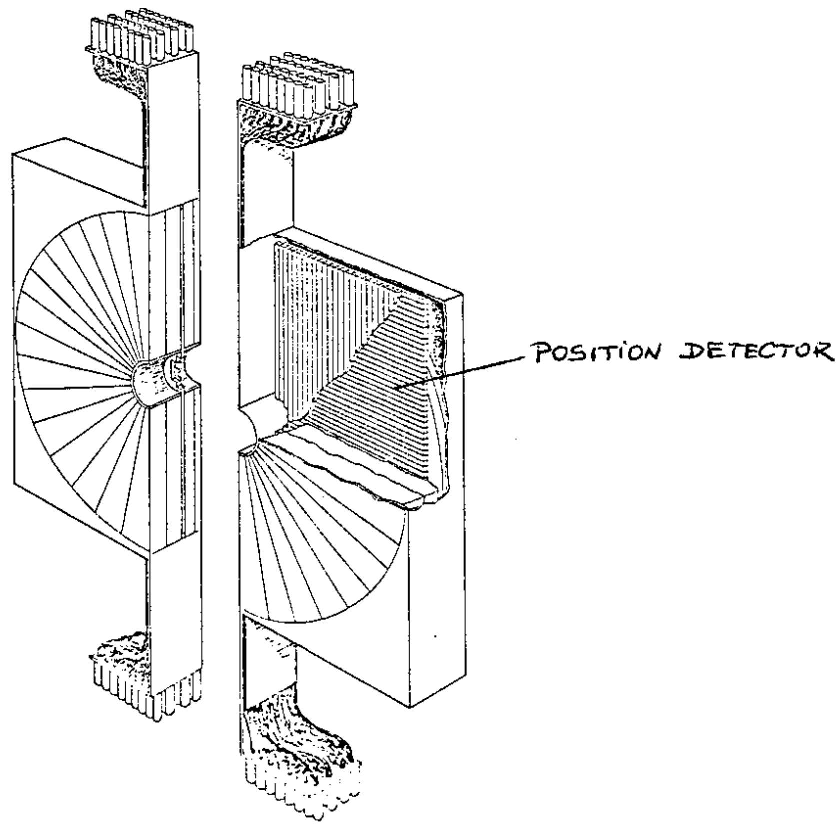
POSITION DETECTOR

Fig. 2

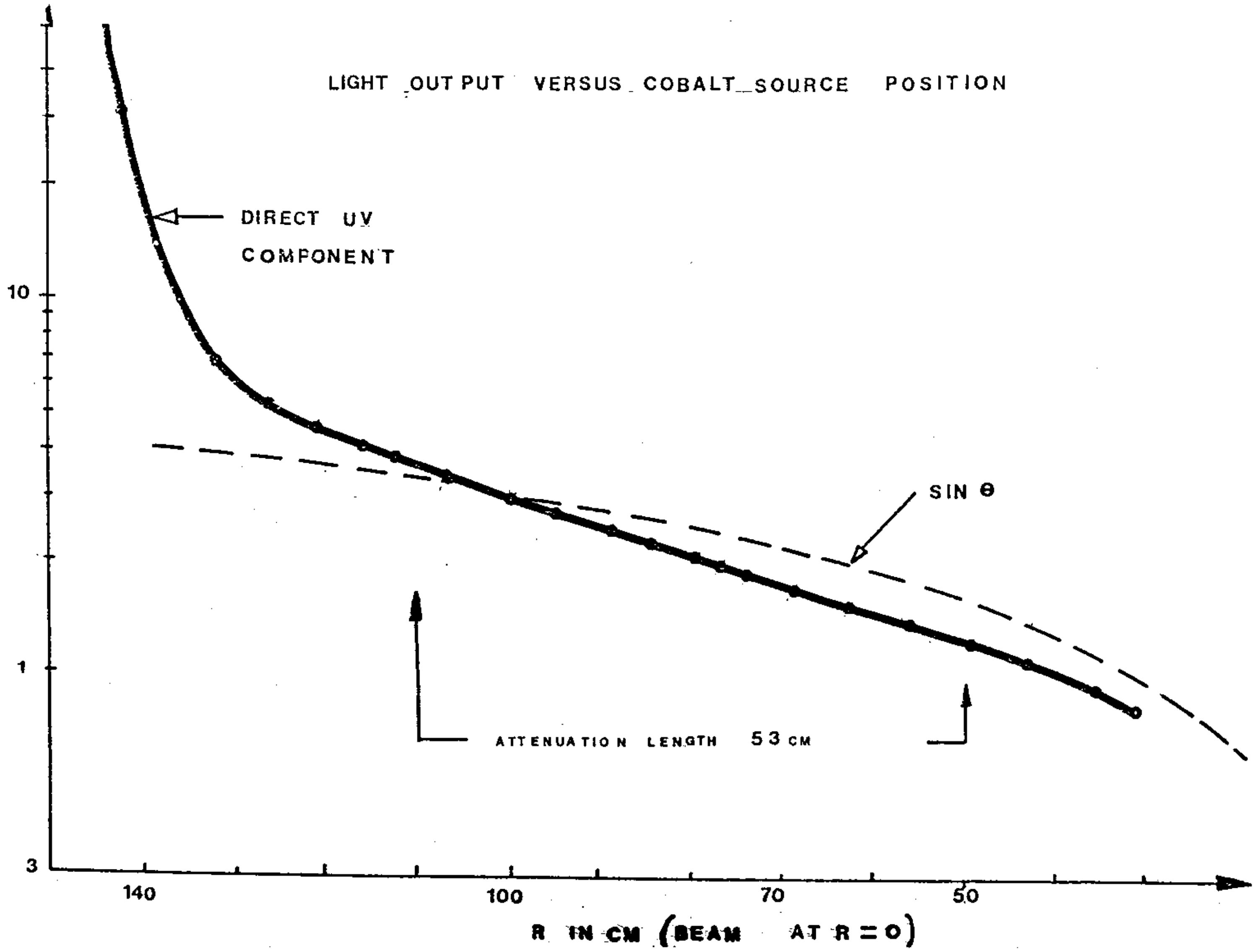
LIGHT OUTPUT VERSUS COBALT SOURCE POSITION
DIRECT UV
COMPONENT
SIN Θ
ATTENUATION LENGTH 53 CM
10
1
3
140
100
70
50
R IN CM (BEAM AT R = 0)

Fig. 3

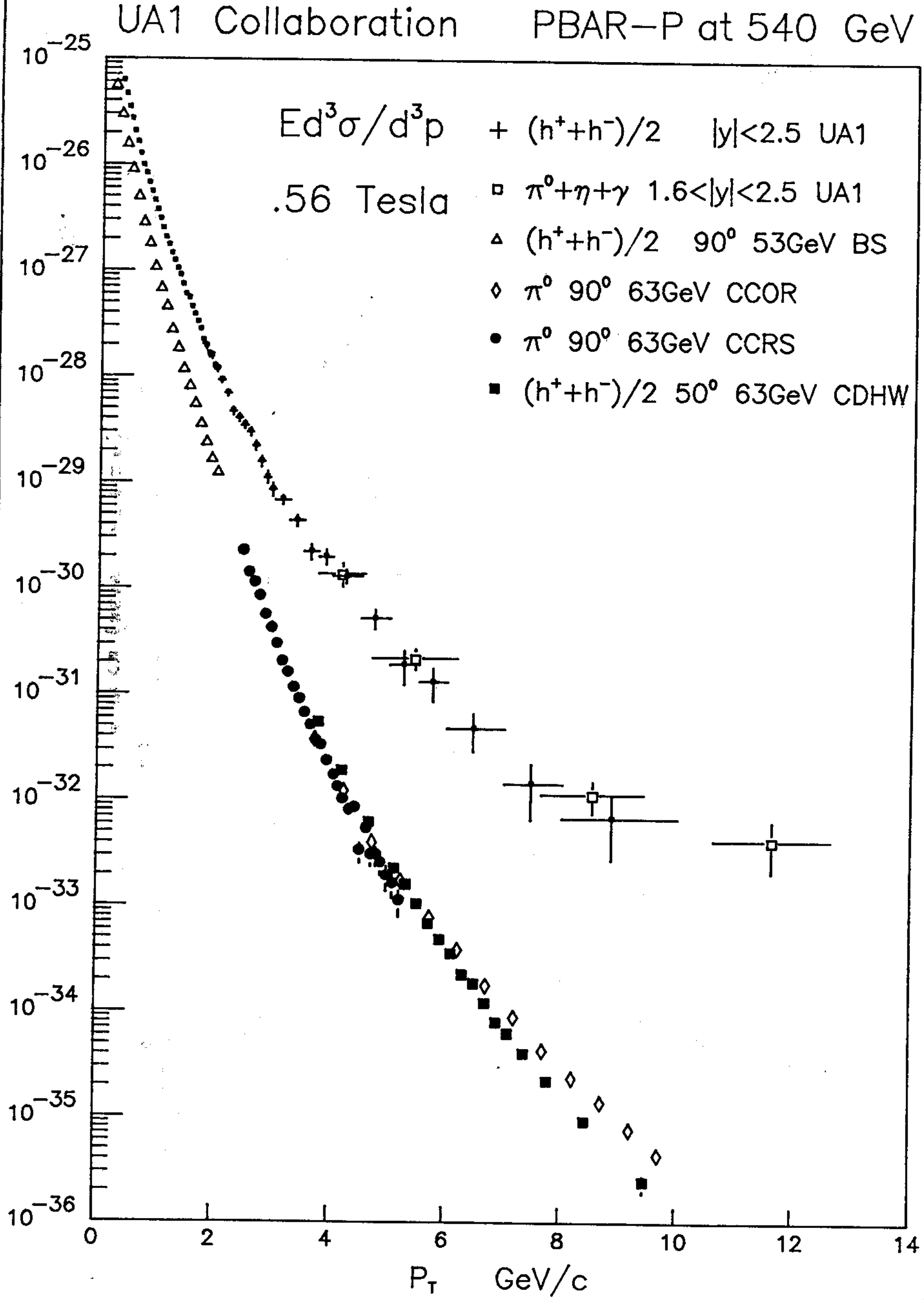
UA1 Collaboration
PBAR−P at 540 GeV
Ed³σ/d³p
.56 Tesla
+ (h⁺+h⁻)/2 |y|<2.5 UA1
□ π⁰+η+γ 1.6<|y|<2.5 UA1
△ (h⁺+h⁻)/2 90° 53GeV BS
◇ π⁰ 90° 63GeV CCOR
● π⁰ 90° 63GeV CCRS
■ (h⁺+h⁻)/2 50° 63GeV CDHW
10⁻²⁵
10⁻²⁶
10⁻²⁷
10⁻²⁸
10⁻²⁹
10⁻³⁰
10⁻³¹
10⁻³²
10⁻³³
10⁻³⁴
10⁻³⁵
10⁻³⁶
0
2
4
6
8
10
12
14
P_T GeV/c

Fig. 4